# Engineering antenna radiation patterns via quasi-conformal mappings

**Carlos García-Meca,[1,*] Alejandro Martínez,[1] and Ulf Leonhardt[2]**

[1]*Nanophotonics Technology Center, Universidad Politécnica de Valencia, Camino de Vera s/n 46022, Valencia, Spain*

[2]*School of Physics and Astronomy, University of St. Andrews, North Haugh, St. Andrews KY16 9SS, United Kingdom*

**cargarm2@ntc.upv.es*

**Abstract:** We use a combination of conformal and quasi-conformal mappings to engineer isotropic electromagnetic devices that modify the omnidirectional radiation pattern of a point source. For TE waves, the designed devices are also non-magnetic. The flexibility offered by the proposed method is much higher than that achieved with conformal mappings. As a result, it is shown that complex radiation patterns can be achieved, which can combine high directivity in a desired number of arbitrary directions and isotropic radiation in other specified angular ranges. In addition, this technique enables us to control the power radiated in each direction to a certain extent. The obtained results are valid for any part of the spectrum. The potential of this method is illustrated with some examples. Finally, we study the frequency dependence of the considered devices and propose a practical dielectric implementation.



**OCIS codes:** (160.3918) Metamaterials; (230.0230) Optical devices.

## References and links

1. A. Martínez, M. A. Piqueras, and J. Martí, "Generation of highly directional beam by k-space filtering using a metamaterial flat slab with a small negative index of refraction," Appl. Phys. Lett. **89**(13), 131111 (2006).
2. A. Martínez, R. García, A. Hakansson, M. A. Piqueras, and J. Sánchez-Dehesa, "Electromagnetic beaming from omnidirectional sources by inverse design," Appl. Phys. Lett. **92**(5), 051105 (2008).
3. J. Li, A. Salandrino, and N. Engheta, "Optical spectrometer at the nanoscale using optical Yagi-Uda nanoantennas," Phys. Rev. B **79**(19), 195104 (2009).
4. Y. Chen, P. Lodahl, and A. F. Koenderink, "Dynamically reconfigurable directionality of plasmon-based single photon sources," Phys. Rev. B **82**(8), 081402 (2010).
5. A. G. Curto, G. Volpe, T. H. Taminiau, M. P. Kreuzer, R. Quidant, and N. F. van Hulst, "Unidirectional emission of a quantum dot coupled to a nanoantenna," Science **329**(5994), 930–933 (2010).
6. D. Dregely, R. Taubert, J. Dorfmüller, R. Vogelgesang, K. Kern, and H. Giessen, "3D optical Yagi-Uda nanoantenna array," Nat Commun **2**, 267 (2011).
7. U. Leonhardt and T. G. Philbin, *Geometry and Light: The Science of Invisibility* (Dover, 2010).
8. F. Kong, B.-I. Wu, J. A. Kong, J. Huangfu, S. Xi, and H. Chen, "Planar focusing antenna design by using coordinate transformation technology," Appl. Phys. Lett. **91**(25), 253509 (2007).
9. W. X. Jiang, T. J. Cui, H. F. Ma, X. Y. Zhou, and Q. Cheng, "Cylindrical-to-plane-wave conversion via embedded optical transformation," Appl. Phys. Lett. **92**(26), 261903 (2008).
10. Y. Luo, J. Zhang, L. Ran, H. Chen, and J. A. Kong, "Controlling the emission of electromagnetic source," PIERS **4**(7), 795–800 (2008).
11. N. Kundtz, D. A. Roberts, J. Allen, S. Cummer, and D. R. Smith, "Optical source transformations," Opt. Express **16**(26), 21215–21222 (2008).
12. B.-I. Popa, J. Allen, and S. A. Cummer, "Conformal array design with transformation electromagnetics," Appl. Phys. Lett. **94**(24), 244102 (2009).
13. P.-H. Tichit, S. N. Burokur, and A. de Lustrac, "Ultradirective antenna via transformation optics," J. Appl. Phys. **105**(10), 104912 (2009).
14. P.-H. Tichit, S. Burokur, D. Germain, and A. de Lustrac, "Design and experimental demonstration of a high-directive emission with transformation optics," Phys. Rev. B **83**(15), 155108 (2011).
15. U. Leonhardt and T. Tyc, "Superantenna made of transformation media," New J. Phys. **10**(11), 115026 (2008).
16. U. Leonhardt, "Optical conformal mapping," Science **312**(5781), 1777–1780 (2006).
17. J. P. Turpin, A. T. Massoud, Z. H. Jiang, P. L. Werner, and D. H. Werner, "Conformal mappings to achieve simple material parameters for transformation optics devices," Opt. Express **18**(1), 244–252 (2010).
18. M. Schmiele, V. S. Varma, C. Rockstuhl, and F. Lederer, "Designing optical elements from isotropic materials by using transformation optics," Phys. Rev. A **81**(3), 033837 (2010).

#152033 - $15.00 USD Received 1 Aug 2011; revised 12 Sep 2011; accepted 16 Sep 2011; published 8 Nov 2011

19. J. Li and J. B. Pendry, "Hiding under the carpet: a new strategy for cloaking," Phys. Rev. Lett. **101**(20), 203901 (2008).
20. Z. Chang, X. Zhou, J. Hu, and G. Hu, "Design method for quasi-isotropic transformation materials based on inverse Laplace's equation with sliding boundaries," Opt. Express **18**(6), 6089–6096 (2010).
21. J. Li, S. Han, S. Zhang, G. Bartal, and X. Zhang, "Designing the Fourier space with transformation optics," Opt. Lett. **34**(20), 3128–3130 (2009).
22. D. Korobkin, Y. Urzhumov, and G. Shvets, "Enhanced near-field resolution in midinfrared using metamaterials," J. Opt. Soc. Am. B **23**(3), 468–478 (2006).
23. J. Valentine, J. Li, T. Zentgraf, G. Bartal, and X. Zhang, "An optical cloak made of dielectrics," Nat. Mater. **8**(7), 568–571 (2009).

## 1. Introduction

During the last decade, a variety of complex structures have been proposed to modify the radiation properties of electromagnetic sources. For instance, a near-zero refractive index slab selects only electromagnetic components impinging with a wave vector perpendicular to its interface, transforming an isotropic source into a highly directional beam [1]. Another approach is the use of photonic crystals, which are able to generate a set of directional beams from an omnidirectional embedded source, since propagation is allowed only in some preferred directions inside the crystal, related to the symmetries of the periodic structure. Moreover, inverse engineering can be employed to modify such periodic structure and achieve a desired radiation pattern that need not be symmetric [2]. In the last few years, plasmonic nanoantennas have also attracted considerable attention, as they enable us to extend many radio antenna concepts to the optical range with devices of reduced size. This includes achieving directional emission patterns, for which most works have focused on Yagi-Uda configurations for different purposes [3–6]. Simultaneously, transformation optics [7] has provided an alternative way to mold the radiation properties of antennas [8–18]. This technique makes it possible to design optical media that make light experience a virtual space, different from the physical one. Points in both spaces (which can be flat or curved) are related by a certain mapping that, together with the metric of those spaces, determines the properties of such optical media [7]. Different transformations have been proposed for a number of applications. These range from the conversion of the cylindrical waves emitted by a line source into four directional beams angularly spaced by 90° [9], to the transformation of more general optical sources that makes them behave as a different virtual source [10–12] and the design of ultra-directive or even invisible antennas [13–15]. The main drawback of this kind of devices is that anisotropic permittivities and permeabilities are required in general, which are difficult to implement.

Recently, the use of conformal transformations [16] has been proposed for antenna engineering [17,18]. Such transformations have the advantage of requiring only isotropic media for their implementation and, for TE polarization (electric field pointing in the direction in which the problem is invariant), only non-magnetic media [7,17,18]. In [17], near-zero constitutive parameters arising from a conformal transformation are employed to transform an isotropic source into one, two or four directional beams. In a more general work, the Schwarz-Christoffel transformation was used to map the circle onto a regular polygon with $N$ sides [18]. The resulting device distributes equally the power of a point source located at the polygon center among $N$ directional beams perpendicular to each polygon side. Thus, these techniques are limited to the design of symmetric antennas radiating in $N$ discrete directions. In this work, we combine this kind of conformal transformations with quasi-conformal mappings to gain more flexibility in the design of radiation-pattern-shaping devices. Although the proposed devices were devised for the optical range, the results are valid for any part of the spectrum. Therefore, normalized distances (in terms of the free-space wavelength $\lambda$) are used throughout the text for the sake of generality.

## 2. Quasi-conformal mappings for antennas

Infinitesimal balls are just scaled and rotated when transformed by a conformal mapping. This is the reason why conformal mappings give rise to isotropic transformation media. Quasi-conformal mappings transform infinitesimal balls to ellipsoids of bounded eccentricity. Thus,

#152033 - $15.00 USD Received 1 Aug 2011; revised 12 Sep 2011; accepted 16 Sep 2011; published 8 Nov 2011

transformation media resulting from a quasi-conformal mapping have a bounded anisotropy that can be neglected if it is small enough. Our goal is to change the omnidirectional radiation pattern of a two-dimensional point source. For this purpose, we will consider the transformation of the unit circle (normalized units) in a flat virtual space to another shape in flat physical space. The functionality of the device will be defined solely by the transformation we apply to the boundary of the considered domain in virtual space (the circle in this case). Thus, we are interested in finding a map that simplifies its implementation. Clearly, a conformal mapping fulfils our requirement as it gives rise to isotropic media. However, except for some specific cases, we do not have at our disposal a conformal transformation mapping the unit circle onto the desired shape. To overcome this problem, we will employ quasi-conformal mappings. Since most algorithms used in the calculation of quasi-conformal mappings transform a rectangular region into other shape, first it is necessary to transform the circle into a rectangle. The best way to do this is by using simple conformal transformations with known analytical expressions. Thus, we will follow a two-step method instead of a direct transformation. First, we will transform the unit circle to a square (with side length $d = 2$) by using a combination of a Möbius transformation mapping the circle to the half upper plane, followed by a Schwarz-Christoffel transformation mapping the half upper plane to the square. The complete transformation is given by Eq. (1):

$$q(w) = \sqrt{-2i}\left(1 - \frac{1}{F\left(\pi/2 \middle| 1/2\right)} F\left(\frac{\pi}{2} - \arcsin\left(w\sqrt{i}\right)\middle|\frac{1}{2}\right)\right). \qquad (1)$$

$F(\varphi|m)$ is the incomplete elliptic integral of the first kind, with amplitude $\varphi$ and parameter $m$. We have expressed this two-dimensional transformation as a function of the complex variable $w = w_1 + iw_2$, with $q = q_1 + iq_2$. The refractive index that implements this transformation can be obtained as $n_1 = |dw/dq|$ [7]. As for the second step, we use a quasi-conformal mapping $z(q_1,q_2) = x + iy$ to transform the square to the desired final shape. The advantage of this kind of quasi-conformal transformations is that they always exist and that, they can be easily calculated numerically. We only need to be careful so that this transformation has a negligible associated anisotropy. For a TE two-dimensional problem, the implementation of the exact quasi-conformal mapping would require a permittivity $\varepsilon = \det(g^{ij})^{-1/2}$ and an anisotropic permeability with in-plane components $\mu_T$ and $\mu_L$ in each of the two principal directions, where $g^{ij}$ is the contravariant metric in the curved coordinates we want to implement [19]. To measure the degree of anisotropy, $\alpha = \max((\mu_T/\mu_L)^{1/2},(\mu_L/\mu_T)^{1/2})$ is usually taken as the anisotropy factor. If $\alpha$ is close to one, $\mu_T \approx \mu_L \approx 1$ and the quasi-conformal mapping can be implemented with negligible error by using only a refractive index distribution $n_2^2 = \varepsilon = \det(g^{ij})^{-1/2}$, as if our mapping were conformal. We will use a simple way of computing such quasi-conformal mappings, which is based on the solution of the inverse Laplace equation supplemented with sliding boundary conditions [20]. In this case, the four sides of the square are mapped to four disjoint specified pieces of the transformed square boundary. The complete transformation refractive index is then given by $n = n_1 n_2$ [7]. In Fig. 1 we illustrate the two steps of this transformation with an example. Conformal maps preserve angles, *i.e.*, two curves meeting at a certain angle in virtual space are mapped to curves in physical space that meet at the same angle. Lines perpendicular to the unit circle boundary will be perpendicular to its transformed counterpart in physical space.

#152033 - $15.00 USD Received 1 Aug 2011; revised 12 Sep 2011; accepted 16 Sep 2011; published 8 Nov 2011

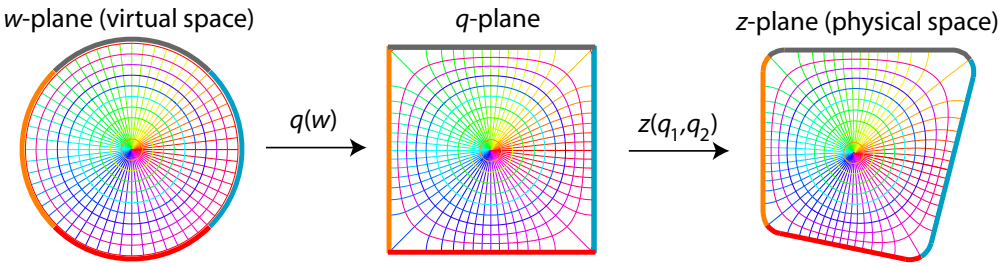


Fig. 1. Mapping of the unit circle to an arbitrary shape by using a conformal transformation $q(w)$ followed by a quasi-conformal one $z(q_1,q_2)$.

Electromagnetic fields follow this transformation, so light rays emanating from a point source located at the center of the unit circle in original space will be normal to the transformed boundary in physical space as well. In order to shape the radiation diagram of the omnidirectional source, we have to orient each little piece of the transformed boundary so that it is perpendicular to the direction towards which we want to redirect the rays crossing that piece. This way we can engineer the angular distribution of the radiated power. This procedure is not exact because of the wave nature of light and the reflections appearing at the transformed circle boundary, since the transformation is not continuous at it. The other limitation is that we do not have full control of the density of rays crossing the transformed circle boundary. We can only decide where to map each fourth of the circle boundary so that we can distribute the radiated power among four desired sets of angular directions, but we cannot specify the angular distribution within each set. Despite the first limitation, the results achieved by this technique are quite accurate. In addition, the second limitation can be overcome to a certain extent as shown below, increasing the degree of control of the angular power distribution.

## 3. Examples

In this section we present three examples illustrating the potential of this technique. We will focus on TE waves so that the resulting devices can be implemented with a gradually changing refractive index distribution. As a first example, imagine that we want to divide the power radiated by the point source into four directional beams, each one propagating in an arbitrary direction. To this end, we should use a quasi-conformal mapping transforming each side of the square to a straight line perpendicular to each of these directions. For instance, let as suppose that those directions correspond to $\theta = 90°$, $\theta = 180°$, $\theta = -20°$, and $\theta = -100°$. In Fig. 2(a) we have depicted a possible choice for the boundary of the final device. Note that we have made use of the flexibility allowed by the quasi-conformal mapping technique in order to avoid steep vertices, which have been rounded. This way, the required refractive index $n$ is always greater than zero. We will also apply this kind of smoothing to the next examples. In Fig. 2(b) we show how the calculated mapping transforms the grid in the $w$-plane depicted in Fig. 1 to the $z$-plane. The refractive index that implements such mapping is included in Fig. 2(c). In this case, $n$ ranges from 0.1 to 1.75, and $\alpha$ is approximately 1.04 so the anisotropy can be neglected. This also applies for the other examples analyzed below, for which similar values of $\alpha$ are obtained. To verify the behavior of the designed devices, we have performed numerical calculations with the commercially available software COMSOL Multiphysics, based on the finite element technique. Isotropic dielectric media have been used in all simulations (anisotropy neglected). In Fig. 2(d) we render the power flow distribution of a point source located in the transformed center of the circle. In addition, we have calculated the far-field distribution $E_{far}(\theta)$ radiated by the system. This enables us to evaluate the directivity, which can be defined as $D = |E_{far}(\theta)/E_{omni}|^2$ for a two-dimensional TE problem, where $E_{omni}$ is the electric far field radiated by a two-dimensional point source in any direction. In Fig. 2(e) we have depicted $D$ in polar coordinates for this first example. We can observe that the radiation pattern consists of four well-defined narrow beams in the desired directions (with a

#152033 - $15.00 USD Received 1 Aug 2011; revised 12 Sep 2011; accepted 16 Sep 2011; published 8 Nov 2011

maximum angle deviation of 0.1°). The directivity in each of these directions is very similar and is higher than 6 (7.8 dB), with a half-power beamwidth BW between 10° and 13°. For comparison purposes, we simulated the exact implementation of the device (anisotropy not neglected). No appreciable differences were observed, as corresponds to small values of $\alpha$.

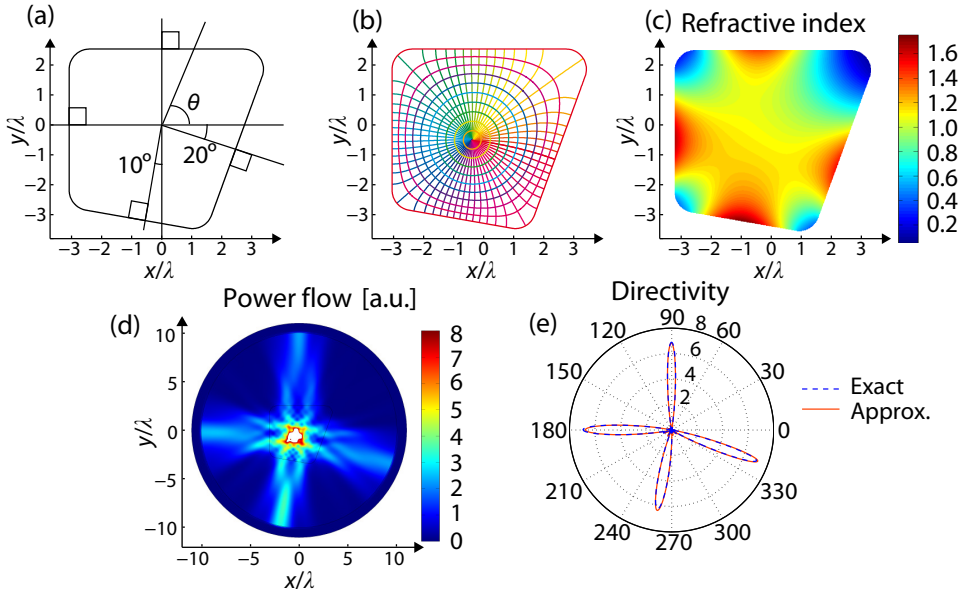


Fig. 2. Control of beam direction: Conversion of an omnidirectional radiation pattern into four narrow beams pointing at any desired direction. (a) Desired boundary of the transformed circle. (b) Resulting quasi-conformal mapping. (c) Refractive index. Simulated (d) power flow, and (e) directivity for the isotropic implementation (red) and exact implementation (blue).

In the second example we show that this technique is not restricted to four-beam antennas and that the power radiated in each direction can be controlled to a certain extent. In this case, imagine that we want to have five beams instead of four, radiating in the directions $\theta = 0°$, $\theta = 90°$, $\theta = 150°$, $\theta = -90°$, and $\theta = -150°$. Moreover, we want the beams associated with the directions $\theta = 150°$ and $\theta = -150°$ to have a smaller directivity than the other ones. These specifications can be accomplished by assigning the left side of the square in the $q$-plane to two segments in the $z$-plane, one of them perpendicular to the direction $\theta = 150°$ and the other one to the direction $\theta = -150°$, while leaving the other three square sides unchanged [Fig. 3(a)]. Since the device is symmetric with respect to the horizontal axis, we know that the beams exiting each of the smaller segments will carry the same power, approximately a quarter of the power carried by each of the other three beams. As in the previous example, the resulting mapping, required refractive index, power flow distribution and directivity are shown in Figs. 3(b)–3(e). The maximum directivity is 3.62 dB for the two secondary lobes and it is between 9.03 dB and 9.2 dB for the main lobes. The refractive index ranges from 0.2 to 1.3.

As a last example, we show that we can also engineer the device to have isotropic radiation within a certain angular range, and not only a set of directional beams. For instance, suppose that we want to have three main lobes radiating in the directions corresponding to $\theta = 0°$, $\theta = 180°$, and $\theta = -90°$, and that we want an isotropic radiation in a 60° angular region defined by the interval $\theta \in [60°, 120°]$. To achieve this, we can transform the upper side of the square in the $q$-plane to a circular boundary, while leaving the other three square sides with the same orientation [see Fig. 4(a)]. This circular boundary must be an arc subtending an angle of 60° in order to distribute the power uniformly in the desired range. According to Fig. 4(a), the radius $r$ of the circle should be $r = 1/\sin(30) = 2$. The mapping, refractive index (varying between 0.2 and 1.32) and directivity are shown in Figs. 4(b)–4(d).

#152033 - $15.00 USD Received 1 Aug 2011; revised 12 Sep 2011; accepted 16 Sep 2011; published 8 Nov 2011

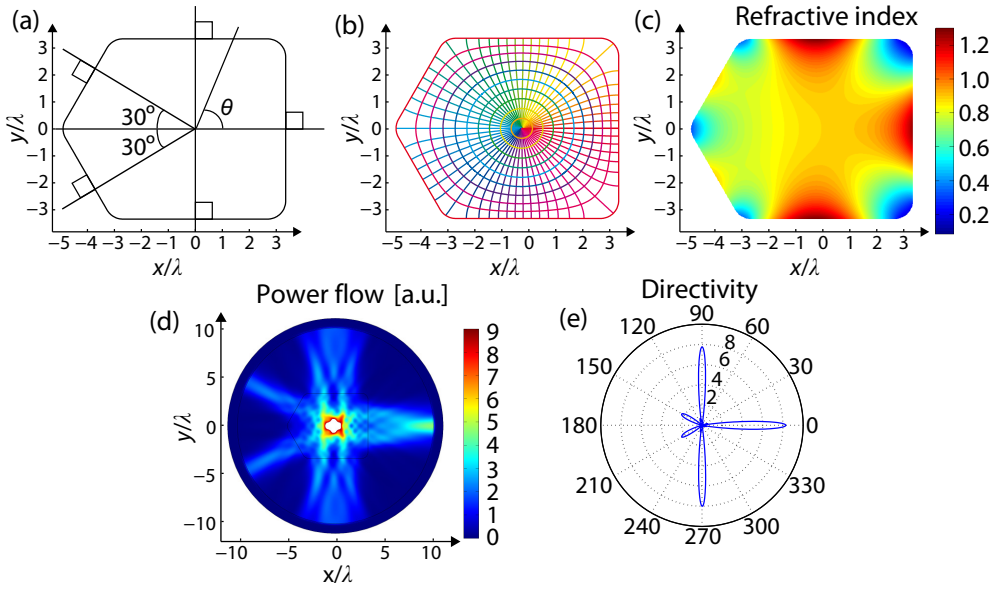


Fig. 3. Control of the number and power of beams: Conversion of an omnidirectional radiation pattern into five narrow beams with different power levels. (a) Desired boundary of the transformed circle. (b) Resulting quasi-conformal mapping. (c) Refractive index. Simulated (d) power flow, and (e) directivity.

For the directional beams, the directivity achieves maximum values of 9.4 dB ($\theta = 0°$ and $\theta = 180°$) and 10.1 dB ($\theta = -90°$), with beamwidths of 9.8°. We have included in Fig. 4(e) a detail of the directivity in the region where we desire an isotropic radiation.

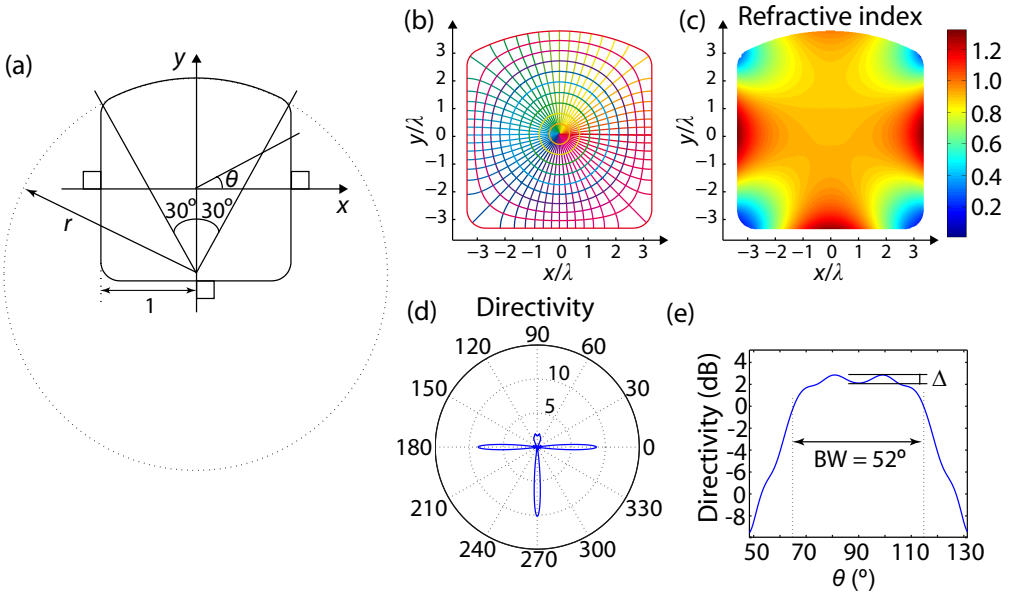


Fig. 4. Generation of a radiation pattern combining high directivity in some directions and isotropic radiation in a desired angular range from an omnidirectional source. (a) Desired boundary of the transformed circle. (b) Resulting quasi-conformal mapping. (c) Refractive index. (d)–(e) Simulated directivity.

There appears a little ripple with amplitude $\Delta \approx 0.7$ dB owing to reflections at the boundary and the fact that the density of rays is higher at the center of the arc, as shown in Fig. 4(b).

#152033 - $15.00 USD Received 1 Aug 2011; revised 12 Sep 2011; accepted 16 Sep 2011; published 8 Nov 2011

Nevertheless, the directivity is higher than 2 dB approximately between 70° and 110° with a beamwidth of around 52°. This last value is somewhat smaller than expected because of the reasons mentioned above and could be corrected by considering a higher angular region in the specifications or by optimizing the radius of curvature of the mapping boundary, which in general could provide a path for engineering a large variety of radiation patterns.

## 4. Frequency dependence and implementation

The performance of the proposed devices should be frequency-independent, provided that non-dispersive materials are employed for their implementation. However, there exists a limiting upper wavelength for which the performance of the device begins to deteriorate significantly. This is due to the fact that we used concepts of ray optics in the design of our device (see discussion above). Thus, its behavior should be closer to the desired one at shorter wavelengths. To analyze the frequency dependence of the proposed devices we focused on the example of Fig. 3. In Figs. 5(a)–5(f) we depict the simulated directivity of this device at different wavelengths. We used the size $d$ of the square side (Fig. 1) as the reference length, since the lateral size of the device is of the order of $d$ (the results in Fig. 3 correspond to $d = 6.6\lambda$). As expected, we observe an improvement of all features at shorter wavelengths. Specifically, for sizes of $d$ larger than $20\lambda$ the performance is optimal, reaching directivities around 13 dB and half-power beamwidths as small as 4°. On the other hand, for $d = 4\lambda$ the secondary lobes do not point at the desired direction and the directivity is quite low. As an approximate rule, we found that the behavior of the device is acceptable for sizes down to $5\lambda$.

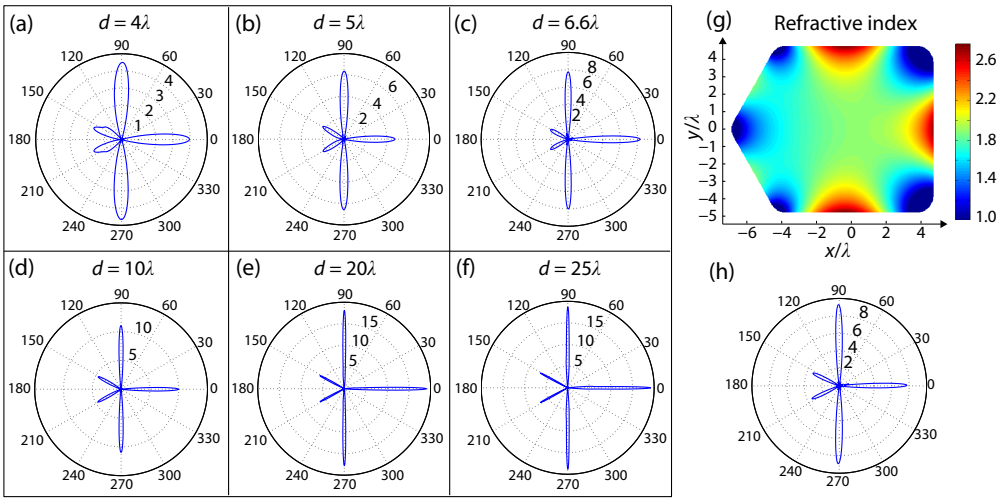


Fig. 5. (a)–(f) Directivity of the device in Fig. 3 at different wavelengths. (g)–(h) Refractive index and directivity of a modified version of the device in Fig. 3.

Regarding the practical realization of the device, the main difficulty stems from the need for refractive indices below unity. Nonetheless, there are several ways to synthesize this kind of media, depending on the wavelength of operation. At optical frequencies, it is possible to use a metal-dielectric composite that, in the effective medium regime, can be regarded as a continuous medium with an effective refractive index between those of the constitutive materials. By spatially changing the filling ratio of both constituents, the desired index profile can be achieved [21]. In addition, there exist natural media that posses a resonant permittivity at some frequencies and could be structured in a similar manner to achieve the sought index distribution. For instance, the permittivity of SiC takes values between zero and one in the midinfrared [22]. At microwaves, the desired properties can be attained by employing metamaterials made up of resonant elements exhibiting effective permittivities lower than unity [14]. In all cases, the desired properties are achieved in a narrow band, either due to the dispersive nature of the employed materials (metals, SiC) or the resonant behavior of the

#152033 - $15.00 USD Received 1 Aug 2011; revised 12 Sep 2011; accepted 16 Sep 2011; published 8 Nov 2011

constituent elements. To solve this problem, we can modify the original device so that the required refractive index is always greater than one and only dielectric materials are required for its implementation. For this purpose, we followed three steps. First, we reduced the size of the transformed circle to raise the resulting refractive index distribution (intuitively, light must travel a shorter distance in the same time, so the refractive index must be larger). Second, we multiplied the whole refractive index distribution by a constant factor $F$. This should not alter the device response in the ray optics approximation, although high values of $F$ could seriously affect its properties. Finally, the refractive index was set to one in the regions where it still was below unity. These regions, as well as $F$, must be small enough so that the device performance is not affected. Continuing with the previous example, a modified version of the device was obtained by reducing its size by a factor of 0.7 and multiplying the resulting index distribution by 1.5. This gave rise to a refractive index distribution greater than one, except in small areas close to the corners, in which the index was set to one. The resulting profile for a device size of the order of $10\lambda$ is shown in Fig. 5(g). It ranges from 1 to 2.7 and could be implemented by milling holes with varying density or size in a dielectric medium [23]. A good directivity is achieved [Fig. 5(h)], somewhat lower than that of the original device [Fig. 5(d)]. It is worth mentioning that the unavoidable discretization of the refractive index profile sets a lower bound for the wavelength of operation, which must be large enough so that the medium is effectively continuous. Despite these limitations, a dielectric implementation should lead to a broadband device, in contrast to the approaches based on photonic crystals or plasmonic nanoantennas, which are usually narrowband due to its resonant nature.

## 5. Conclusions

We have shown how to engineer antenna radiation patterns in several ways with the aid of quasi-conformal mappings that result in isotropic and non-magnetic devices. As compared to previous works based on conformal transformations this technique provides us with a higher degree of control, allowing us to divide the power into highly directional beams in a set of desired directions and isotropic radiation in other angular ranges. More complex radiation patterns could be achieved by combining the presented ideas. The flexibility offered by quasi-conformal mappings enables us to avoid zero-index regions. In addition, we have analyzed the frequency dependence of the proposed devices, finding that they behave well for lateral sizes down to $5\lambda$. Finally, we have proposed a feasible implementation that only requires isotropic dielectric media with refractive index values above unity.

## Acknowledgments

Financial support by the Spanish Ministerio de Ciencia e Innovación (contract CSD2008-00066 and FPU grant) is gratefully acknowledged.

#152033 - $15.00 USD Received 1 Aug 2011; revised 12 Sep 2011; accepted 16 Sep 2011; published 8 Nov 2011